

Fabrication and high photocatalytic activity of TiO₂ microspheres formed by surfactant assisted polymerization-induced colloid aggregation

ZHONGYU LI^{a,b*}, YONGLING FANG^a, SONG XU^{a*}, DANDAN HAN^b, DAYONG LU^b

^aJiangsu Key Laboratory of Advanced Catalytic Materials and Technology, Department of Petrochemical Engineering, Changzhou University, Changzhou 213164, PR China

^bDepartment of Material Science and Chemical Engineering, Jilin Institute of Chemical Technology, Jilin 132022, PR China

TiO₂ microspheres were successfully prepared via an improved polymerization-induced colloid aggregation (PICA) process assisted by surfactant. The as-prepared sample was characterized by XRD, SEM, TEM, Raman spectroscopy and nitrogen adsorption-desorption isotherms. The characterization results indicate that as-prepared TiO₂ microspheres are the mixture of anatase and rutile phases. The specific surface area and porosity of the sample were evaluated using Brunauer-Emmett-Teller (BET) method and Barrett-Joyner-Halenda (BJH) models. The photocatalytic activity of the TiO₂ microspheres was investigated by degrading the different target contaminants, including methyl blue (MB), methyl orange (MO) and rhodamine B (RhB) under UV light irradiation. The photocatalytic studies show that the MB, MO and RhB have been almost completely degraded and mineralized after 25 min, 70 min and 140 min of UV light irradiation, respectively. The photocatalytic degradation rate of as-prepared TiO₂ microspheres show comparative capacity compared with TiO₂-P25. These results indicate the TiO₂ microspheres exhibit high photocatalytic activity.

(Received January 21, 2013; accepted September 18, 2013)

Keywords: Titanium dioxide, TiO₂ microspheres, PICA process, Photocatalytic activity, Colloidal processing

1. Introduction

The efficient treatment of industrial wastewaters and contaminated drinking water sources has become of great importance in a world that is facing with ever increasing population and decreasing energy resources. Since Fujishima and Honda reported the evolution of oxygen and hydrogen from a titanium dioxide (TiO₂) electrode under the irradiation of light in 1972 [1], semiconductor photocatalytic technique has shown a great potential as a low-cost, environmentally friendly, and sustainable treatment technology to align with the “zero” waste scheme in the water/wastewater industry [2-5].

Of the many different photocatalysts, titanium dioxide, due to its excellent chemical stability, non-toxicity and low cost, has been widely studied as a promising semiconductor photocatalyst for potential application in photocatalytic degradation of organic pollutants [6-13]. Among the TiO₂ based photocatalysts, spherical TiO₂ particles are one of the most studied materials because of their geometric structure and specific properties, such as high specific surface area and low rate of charge carrier recombination [14-16]. These features can increase the light-harvesting capabilities of the spherical TiO₂ particles, which make TiO₂ nano/microspheres exhibit excellent

photocatalytic performance [17-19]. Various physicochemical and chemical methods have been developed to prepare hollow and porous TiO₂ nano/microspheres [20-26].

Recently, a polymerization-induced colloid aggregation (PICA) strategy was developed for the fabrication of hierarchical porous materials [27,28]. In this procedure, the colloid of the target material (gotten by hydrolysis process or by suspending the pre-prepared nanoparticles in solution) first formed inorganic-organic hybrid with monomers/oligomer and the polymerization of the monomer/oligomer induced the aggregation of the colloid. The removal of the polymer produced hierarchical porous inorganic materials. Obviously, the PICA strategy is more controllable method for the synthesis of porous transition metal oxides. Shi et al. [27] obtained the zeolite microspheres with hierarchical porous structure through an improved PICA process with the urea-formaldehyde resin. Mao et al. [28] reported the fabrication of bimodal mesoporous hematite microspheres with the aid of polymerization of acrylamide-directed aggregation. In the present study, the TiO₂ microspheres were synthesized using a surfactant assisted polymerization-induced colloid aggregation process, larger specific surface area of 48.1 m²/g have been achieved compared with the original PICA

method of 36.7 m²/g [29] which suggested more active sites on the surface of TiO₂ nanoparticles may induced higher photocatalytic activity. What's more, photocatalytic activity of TiO₂ samples was evaluated by measuring photodegradation of different dyes compared to the traditional TiO₂-P25.

2. Experimental

2.1. Preparation of TiO₂ microspheres

30 ml of deionized water and 2 ml of concentrated hydrochloric acid were placed into a three-necked flask equipped with a mechanical stirrer and a thermometer. Then 7 ml of tetra-n-butyl titanate was added drop-wise to the acid solution and heated to 60 °C until the flocky precipitate disappeared to form a uniform solution. After the sol solution was cooled down to room temperature, 0.15 g of sodium dodecyl sulfate (SDS), 2.1 g of urea and 10 ml of formaldehyde solution (37%) were added with continuous stirring. The mixture was stirred for 20 h at room temperature, and then kept static for 1 h. The obtained precipitate was filtered, washed with deionized water repeatedly, and then dried. As-synthesized urea-formaldehyde resin/titanium hydroxide composites were calcined at 500 °C in air for 3 h to yield TiO₂ microsphere.

2.2. Characterization

X-ray diffraction (XRD) measurements were carried out at room temperature using a Rigaku D/MAX-2500PC diffractometer (Rigaku Co., Japan) with Cu K_α radiation ($\lambda=0.15406$ nm) operated at 40 kV and 100 mA. The morphologies of the samples were observed on a JEM-2100 transmission electron microscopy (TEM, JEOL, Japan) and JSM-6360LA scanning electron microscopy (SEM, JEOL, Japan). Raman spectra were measured at room temperature using a LabRAM XploRA Raman spectrometer (Horiba Jobin Yvon, France) with a 532 nm laser focused on a spot of about 3 nm in diameter. Nitrogen adsorption-desorption isotherms were measured using an Autosorb-iQ2-MP apparatus (Quantachrome Co., US), the BET (Brunauer-Emmett-Teller) method and BJH (Barrett-Joyner-Halenda) models were used for specific surface area calculation and porosity evaluation, respectively.

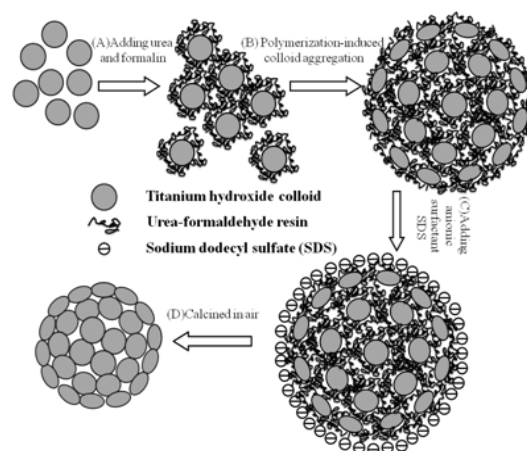
2.3. Photocatalytic activity

The photocatalytic activity of TiO₂ microspheres was evaluated by photodegradation of the different target contaminants, including methyl blue (MB), methyl orange (MO) and rhodamine B (RhB). The photocatalytic experiments were carried out by adding 10 mg TiO₂ powder into cylindrical glass vessel with a circulating water jacket containing 50 ml of the target contaminant

aqueous solution. Before irradiation of UV light, the suspension containing the target contaminant and photocatalysts was continuously stirred in dark for 30 minutes in order to reach an adsorption-desorption equilibrium. After that, the suspension was irradiated while stirring by UV light which was obtained by a 500 W highly pressure mercury vapor lamp. During irradiation, each sample for analysis was taken out at regular intervals. The TiO₂ particles were taken from the mixture solution with centrifugation at 5000 rpm for 20 min. The clarified solution was analyzed by UV759 UV-vis spectrometer (Shanghai Precision & Scientific Instrument Co., Ltd., China) to obtain the absorbance of the target contaminant at their maximum absorption wavelength. The degradation rate (D) of the target contaminant could be calculated by $D = (1 - C_t/C_0) \times 100\%$, where C_0 is the concentration of the target contaminant after darkness absorption for 30 min and C_t is the concentration of the target contaminant at time t .

3. Results and discussion

The TiO₂ microspheres were synthesized by surfactant assisted polymerization-induced titanium hydroxide colloid aggregation as shown in Scheme 1. Titanium hydroxide colloid was first prepared by tetra-n-butyl titanate and hydrochloric acid, and then urea and formalin were added. The polymerization of urea and formalin could induce the condensation of titanium hydroxide colloids, the composites of urea-formaldehyde resin and titanium hydroxide were obtained. Adding anionic surfactant SDS is to form an electronegative microcapsule reaction environment to protect hybrid polymerization process effectively. At last the urea-formaldehyde resin and SDS were removed by calcination to yield TiO₂ microspheres.



Scheme 1 Schematic illustration of the preparation of TiO₂ microspheres.

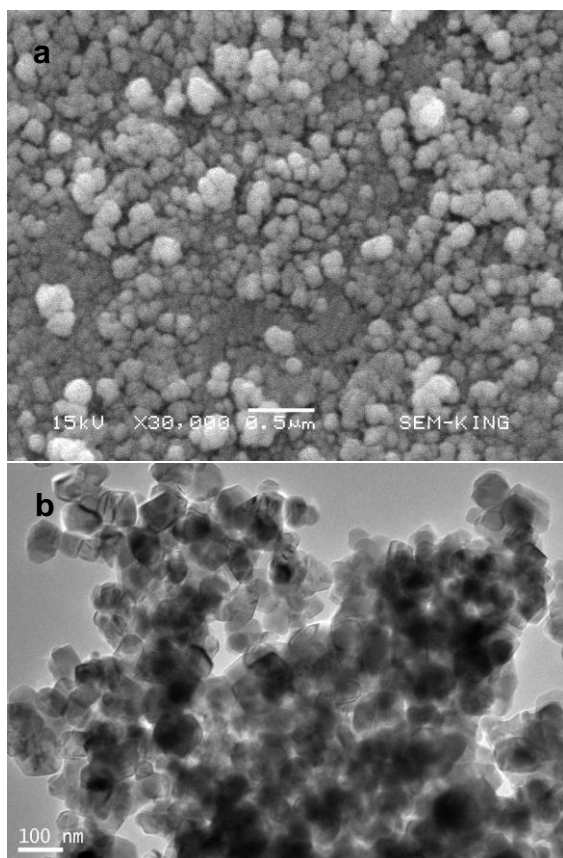


Fig. 1. SEM image (a) and TEM image (b) of the TiO_2 microspheres.

The SEM image of the as prepared TiO_2 microspheres is shown in Fig. 1a. The diameter of the TiO_2 microspheres is about 90-120 nm. The TiO_2 microspheres possess a relatively narrow particle size distribution with relatively uniform spherical. Although the influence of thermal treatment temperature induced slight agglomeration, better dispersity of obtained TiO_2 microspheres can be achieved than the commercial TiO_2 -P25 [30]. Fig. 1b presents the TEM image of the as prepared TiO_2 microspheres. The diameter of the TiO_2 microspheres is about 80-110 nm, which is almost in agreement with the SEM result.

The XRD pattern of TiO_2 microspheres is shown in Fig. 2. The TiO_2 microspheres contain a mixture of anatase and rutile phases. The characteristic diffraction peaks at $2\theta = 25.3, 37.8, 48.0, 54.3$ and 62.7° can be assigned to (101), (004), (200), (105) and (204) crystal plane of anatase TiO_2 (JCPDS Card No. 01-0562), while diffraction peaks at $27.4, 36.0, 41.2, 56.6$ and 68.9° can be assigned to (110), (101), (111), (220) and (301) crystal plane of rutile TiO_2 (JCPDS Card No.75-1757). The reflection peaks are very sharp, indicating the obtained TiO_2 has a good crystallinity. The average crystallite size was calculated from the major diffraction peak (101) of the anatase phase to be approximately 13 nm. Furthermore, the mixture of anatase and rutile phases seems to guarantee the occurrence of

crystal defects that can slow the natural recombination of charge carriers, which be proved to has higher photocatalytic activity by Hu and Zhang [31].

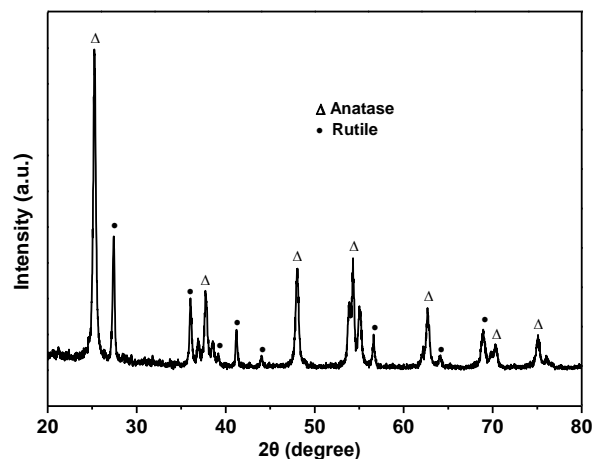


Fig. 2. X-ray diffraction patterns of the TiO_2 microspheres.

The Raman spectrum of the TiO_2 microspheres is shown in Fig. 3. According to factor group analysis, anatase has six Raman active modes ($A_{1g}+2B_{1g}+3E_g$).

The Raman spectrum of an anatase single crystal has been investigated by Ohsaka et al. [32], who concluded that the six allowed modes appear at 144 cm^{-1} (E_g), 197 cm^{-1} (E_g), 399 cm^{-1} (B_{1g}), 513 cm^{-1} (A_{1g}), 519 cm^{-1} (B_{1g}) and 639 cm^{-1} (E_g). In the case of rutile, the fundamental modes are 143 cm^{-1} (B_{1g}), 447 cm^{-1} (E_g), 612 cm^{-1} (A_{1g}) and 826 cm^{-1} (B_{1g}); the most intensive bands are E_g and A_{1g} , the low frequency one (B_{1g}) is the narrowest [33]. It can be observed from Fig. 3, the Raman peaks at 148.13 cm^{-1} , 199.69 cm^{-1} , 400.78 cm^{-1} , 519.38 cm^{-1} and 641.41 cm^{-1} are characteristics of the anatase phase, while 448.91 cm^{-1} and 612.19 cm^{-1} are characteristics of the rutile phase of TiO_2 . It was proved that the as-prepared TiO_2 microspheres contain the mixture of anatase and rutile crystals.

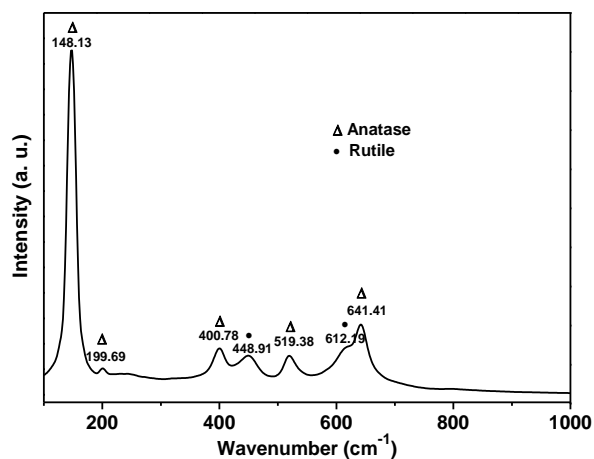


Fig. 3. Raman spectrum of the TiO_2 microspheres.

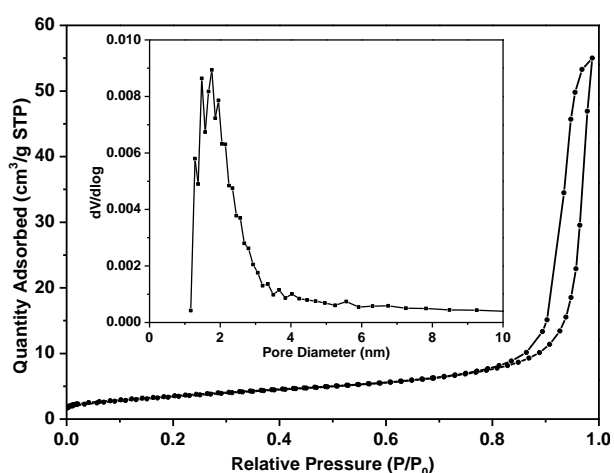


Fig. 4. Nitrogen adsorption-desorption isotherms and the pore diameter distribution (inset) of the TiO₂ microspheres.

The nitrogen adsorption-desorption isotherms of TiO₂ microspheres are illustrated in Fig. 4. The isotherm corresponding to TiO₂ microspheres is type IV curve [34]. The hysteresis loop observed at relative pressures ($P/P_0 = 0.8-1.0$) is indicative of existing mesopores in the obtained TiO₂ microspheres. The inset of Fig. 4 shows the pore-diameter distribution evaluated by the Barrett-Joyner-Halenda (BJH) method. The BJH pore size distribution shows a maximum at 1.8 nm close to the limit between micropores and mesopores (2.0 nm) with a significant contribution above 2.0 nm. By calculation, the BET surface specific area of TiO₂ sample reaches to be 48.1 m²/g, which is similar with the conventional and pervasive TiO₂-P25 of 47.57 m²/g specific area [35].

Fig. 5 shows the photocatalytic activity of TiO₂ microparticles on decomposition of the target contaminants (MB, MO and RhB) under UV light irradiation. It can be seen from Fig. 5a, the decrease of absorption peak of MB at 665 nm indicates a rapid degradation of the dye. Moreover, the absorption maximum wavelength shifts from 665 nm to 607 nm during irradiation. After 25 min of UV light irradiation, almost no other spectral features are evident in the absorption spectra, indicating that the MB was almost completely degraded and mineralized by the TiO₂ microspheres. While, the MO and RhB were almost completely degraded and mineralized after 70 min and 140 min of UV light irradiation, respectively (Fig. 5b and 5c). To take the process of MB decomposition for an example in Fig. 5d, compared with the traditional and commercial catalytic TiO₂-P25, the as-prepared TiO₂ microspheres exhibited almost same considerable photocatalytic degradation capacity of approximately 100% removal rate with 25 min UV light irradiation while the self-degradation rate of MB is merely 11% which demonstrated that TiO₂ photocatalyst play an important role in the process of MB decomposition under ultraviolet light illumination.

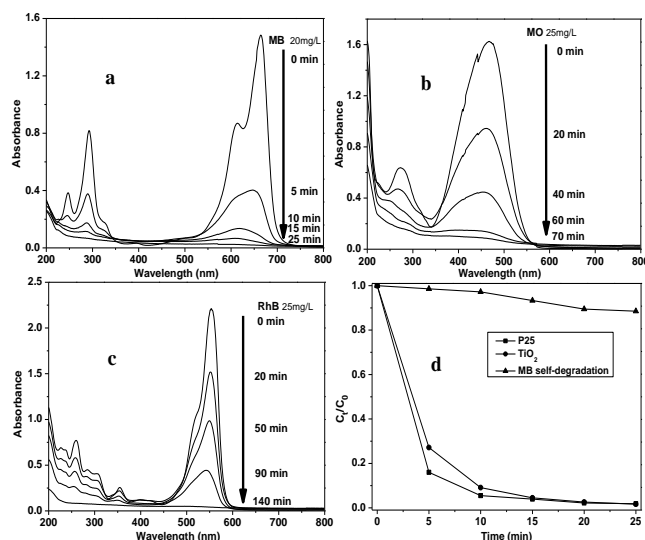


Fig. 5. Temporal changes in absorption spectra of MB solution (a), MO solution (b) and RhB solution (c) under UV light irradiation; (d) Photocatalytic degradation of MB in the presence of P25, as-prepared TiO₂ and absence of catalysis.

The UV light induced photocatalytic mechanism in the presence of TiO₂ microspheres was shown in Fig. 6. After UV light irradiation, electrons (e^-) are excited from the valence band (VB) to the conduction band (CB) of TiO₂ while leaving holes (h^+) in the VB. When the energy of the photons matches or exceeds the band gap energy of TiO₂ (3.2 eV), the electron-hole pairs were formed. In the process of degrading and mineralizing organic pollutants, the radicals such as $\cdot O_2^-$ and $\cdot OH$ were generated when the e^- and h^+ pairs react with a stable electron acceptor and donor [36]. With a series process of photoexcitation, photoinduction and recombination of electrons and holes, various oxidation-reduction reactions were taken place on the TiO₂ surface, the MB molecules were easy to degrade and mineralize to the degradation product.

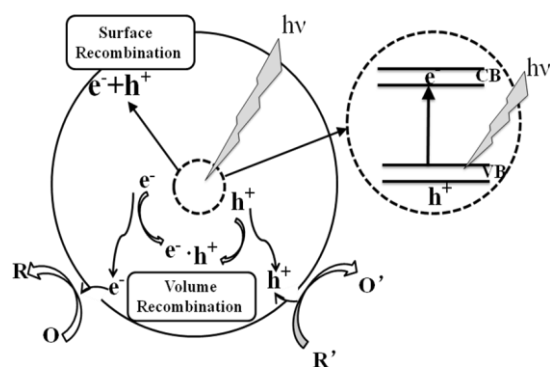


Fig. 6. Schematic diagram of possible UV light induced photocatalytic mechanism in the presence of TiO₂ microspheres.

4. Conclusion

The TiO₂ microspheres were fabricated via an improved PICA method assisted by surfactant. The as-prepared sample was characterized by XRD, SEM, TEM, Raman spectroscopy and nitrogen adsorption-desorption isotherms. The XRD patterns and Raman spectrum indicate that the TiO₂ microspheres are a mixture of anatase and rutile crystals, which possesses the higher photocatalytic activity. Based on the BET results, the TiO₂ nanoparticles we obtained possess larger specific area compared with the classical and commercial TiO₂-P25, and more active sites could give rise to higher photocatalytic activity. The photocatalytic experiments proved that the as-prepared TiO₂ microspheres exhibited high photocatalytic activity in agreement with P25 under UV light irradiation.

Acknowledgements

This work was supported by the Research Foundation for Talented Scholars of Changzhou University (ZMF11020007), Project for Six Major Talent Peaks of Jiangsu Province (2011-XCL-004), Natural Science Foundation of Changzhou City (CJ20115009) and Research and Innovation Project for College Graduates of Jiangsu Province (CXLX-0711).

References

- [1] A. Fujishima, K. Honda, *Nature* **5358**, 37 (1972).
- [2] M. A. Fox, M.T. Dulay, *Chem. Rev.* **93**, 341 (1993).
- [3] D. Wang, J. Zhang, Q. Z. Luo, X. Y. Li, Y. D. Duan, J. An, *J. Hazard. Mater.* **169**, 546 (2009).
- [4] X. Z. Li, H. Liu, L. F. Cheng, H. J. Tong, *Environ. Sci. Technol.* **37**, 3989 (2003).
- [5] T. S. Jamil, M. Y. Ghaly, N. A. Fathy, T. A. Abd el-halim, L. Österlund, *Sep. Purif. Technol.* **98**, 270 (2012).
- [6] D. Y. Choi, J. Y. Park, J. W. Lee, *Mater. Lett.* **89**, 212 (2012).
- [7] M. N. Blanco, L. R. Pizzio, *Appl. Surf. Sci.* **256**, 3546 (2010).
- [8] G. H. Jiang, X. Y. Zheng, Y. Wang, T. W. Li, X. K. Sun, *Powder Technol.* **207**, 465 (2011).
- [9] M. Behpour, V. Atouf, *Appl. Surf. Sci.* **258**, 6595 (2012).
- [10] A. Zyoud, N. Zaatar, I. Saadeddin, M. H. Helal, G. Campet, M. Hakim, D. H. Park, H. S. Hilal, *Solid State Sci.* **13**, 1268 (2011).
- [11] Z. Y. Wang, W. P. Mao, H. F. Chen, F. A. Zhang, X. P. Fan, G. D. Qian, *Catal. Commun.* **7**, 518 (2006).
- [12] Q. Q. Wang, S. H. Xu, F. L. Shen, *Optoelectron. Adv. Mater. – Rapid Comm.* **5**, 128 (2011).
- [13] Z. Chen, Z. Zhang, Z. Zhong, C. Zhang, J. Xu, *Optoelectron. Adv. Mater. – Rapid Comm.* **5**, 398 (2011).
- [14] S. W. Liu, J. G. Yu, M. Jaroniec, *J. Am. Chem. Soc.* **132**, 11914 (2010).
- [15] S. Liu, X. Sun, J. G. Li, X. Li, Z. Xiu, H. Yang, X. Xue, *Langmuir* **26**, 4546 (2010).
- [16] G. K. Mor, K. Shankar, M. Paulose, O. K. Varghese, C. A. Grimes, *Nano. Lett.* **6**, 215 (2006).
- [17] F. Jiang, S. R. Zheng, L. C. An, H. Chen, *Appl. Surf. Sci.* **258**, 7188 (2012).
- [18] S. M. Klein, V. N. Manoharan, D. J. Pine, F. F. Lange, *Langmuir* **21**, 6669 (2005).
- [19] S. Pazokifard, S.M. Mirabedini, M. Esfandeh, S. Farrokhpay, *Adv. Powder Technol.* **23**, 428 (2012).
- [20] J. Xie, D. Jiang, M. Chen, D. Li, J. Zhu, X. Lu, C. Yan, *Colloid Surf. A*, **372**, 107 (2010).
- [21] T. Prakash, M. Navaneethan, J. Archana, S. Ponnusamy, C. Muthamizhchelvan, Y. Hayakawa, *Mater. Lett.* **82**, 208 (2012).
- [22] X. Xiong, M. Lin, J. Duan, Y. Wang, Z. Yu, *React. Func. Polym.* **72**, 365 (2012).
- [23] J. B. Fei, Y. Cui, X. H. Yan, W. Qi, Y. Yang, K. W. Wang, Q. He, J. B. Li, *Adv. Mater.* **20**, 452 (2008).
- [24] H. X. Li, Z. F. Bian, J. Zhu, D. Q. Zhang, G. S. Li, Y. N. Huo, Y. F. Lu, *J. Am. Chem. Soc.* **129**, 8406 (2007).
- [25] H. Pan, J. S. Qian, Y. M. Cui, H. X. Xie, X. F. Zhou, *J. Mater. Chem.* **22**, 6002 (2012).
- [26] D. H. Chen, L. Cao, T. L. Hanley, R. A. Caruso, *Adv. Func. Mater.* **22**, 1966 (2012).
- [27] Y. Shi, X. Li, J. K. Hu, J. H. Lu, Y. C. Ma, Y. H. Zhang, Y. Tang, *J. Mater. Chem.* **21**, 16223 (2011).
- [28] D. Mao, J. Yao, X. Lai, M. Yang, J. Du, D. Wang, *Small* **7**, 578 (2011).
- [29] Z. T. Jiang, Y. M. Zuo, *Anal. Chem.* **73**, 686 (2001).
- [30] X. B. Chen, S. S. Mao, *Chem. Rev.* **107**, 2891 (2007).
- [31] H. Xu, L. Z. Zhang, *J. Phys. Chem. C* **113**, 1785 (2009).
- [32] T. Ohsada, F. Izumi, Y. Fujiki, *J. Raman Spectrosc.* **7**, 321 (1978).
- [33] S. P. S. Porto, P. A. Fleury, T. C. Damen, *Phys. Rev.* **154**, 522 (1967).
- [34] J. G. Yu, S. W. Liu, H. G. Yu, *J. Catal.* **249**, 59 (2007).
- [35] H. Zhang, X. J. Lv, Y. M. Li, Y. Wang, J. H. Li, *ACS Nano* **4**, 380 (2010).
- [36] Z. Y. Li, Y. L. Fang, X. Q. Zhan, S. Xu, *J. Alloys Compd.* **564**, 138 (2013).

*Corresponding author: zhongyuli@mail.tsinghua.edu.cn;
cyanine123@163.com